ISSN 0208-7774 TRIBOLOGIA 4/2020 p. 27–36
DOI: 10.5604/01.3001.0014.5895

Dariusz OZIMINA[*], Katarzyna PIOTROWSKA[**], Monika MADEJ[***], Arkadiusz GRANEK[****]

THE INFLUENCE OF ION IMPLANTATION ON THE PROPERTIES OF Ti6Al4V TITANIUM ALLOY IN BIOTRIBOLOGICAL SYSTEMS

WPŁYW IMPLANTACJI JONOWEJ NA WŁAŚCIWOŚCI STOPU TYTANU Ti6Al4V W SYSTEMACH BIOTRIBOLOGICZNYCH

Key words: ion implantation, titanium alloys, SEM, friction, wear, surface texture.

Abstract: The article is devoted to the assessment of the geometrical structure of the surface as well as the mechanical and tribological properties of the surface layers obtained in the process of ion implantation. The titanium alloy Ti6Al4V used in biotribological systems was implanted with nitrogen and argon ions. Investigations of the geometrical structure of the surface before and after the tribological tests were carried out using confocal microscopy. The hardness of the tested materials was determined by the instrumental indentation method using a Vickers indenter. A nanotribometer was used for tribological tests. The tests were carried out in a reciprocating motion under conditions of technically dry friction and friction with the lubrication of Ringer's solution. SEM scanning microscopy was used to determine the width of the wear pattern and the wear mechanism. The conducted research showed that the hardness of the tested materials increased as a result of ion implantation. The tribological tests showed that the use of ion implantation improves the tribological properties, and the dominant wear mechanism was abrasive wear.

Słowa kluczowe: implantacja jonowa, stopy tytanu, SEM, tarcie, zużycie, struktura geometryczna powierzchni.

Streszczenie: Artykuł poświęcony jest ocenie struktury geometrycznej powierzchni oraz właściwości mechanicznych i tribologicznych warstw wierzchnich uzyskiwanych w procesie implantacji jonowej. Stop tytanu Ti6Al4V stosowany systemach biotribologicznych implantowano jonami azotu i argonu. Badania struktury geometrycznej powierzchni przed i po testach tribologicznych przeprowadzano przy użyciu mikroskopii konfokalnej. Twardość badanych materiałów wyznaczano metodą instrumentalnej indentacji przy zastosowaniu wgłębnika Vickersa. Do testów tribologicznych wykorzystano nanotribometr. Badania realizowano w ruchu posuwisto-zwrotnym w warunkach tarcia technicznie suchego oraz tarcia ze smarowaniem roztworem Ringera. Mikroskopię skaningową SEM wykorzystano do określenia szerokości śladu wytarcia oraz mechanizmu zużywania. Przeprowadzone badania wykazały, że w wyniku implantacji jonowej nastąpił wzrost twardości badanych materiałów. Testy tribologiczne wskazały, że zastosowanie implantacji jonowej wpływa na poprawę właściwości tribologicznych, a dominującym mechanizmem zużywania było zużycie ścierne.

INTRODUCTION

Biomedical materials are widely used in medicine from the simple products with the lowest risk for the patient (e.g., orthopaedic collars), increased risk, up to invasive, remaining in the human body for a long time (often for life) and carrying a very high risk for the patient, such as joint implants or heart valves. They are also used in diagnostics and for surgical instruments. Contemporary biomaterials must meet high requirements, e.g.,

[*] ORCID: 0000-0001-5099-6342. Kielce University of Technology, Faculty of Mechatronics and Mechanical Engineering, Tysiąclecia Państwa Polskiego 7 Ave., 25-314 Kielce, Poland.
[**] ORCID: 0000-0001-6366-2755. Kielce University of Technology, Faculty of Mechatronics and Mechanical Engineering, Tysiąclecia Państwa Polskiego 7 Ave., 25-314 Kielce, Poland.
[***] ORCID: 0000-0001-9892-9181. Kielce University of Technology, Faculty of Mechatronics and Mechanical Engineering, Tysiąclecia Państwa Polskiego 7 Ave., 25-314 Kielce, Poland.
[****] Hospital MSWiA, Ogrodowa 11 Street, 25-024 Kielce, Poland.

they must have very good mechanical parameters, biocompatibility, and resistance to tribological wear and corrosion **[L. 1, 2]**.

The use of titanium and its alloys for components of medical implants is well known. It is due to its biocompatibility and mechanical and corrosive properties. Due to the high biocompatibility of these materials with living organisms, the phenomenon of osseointegration (bone connection with the surface of the implant) quickly occurs at the border between the implant and the bone tissue. The limitation in the use of titanium for medical implants is the relatively low wear resistance; and, in the case of alloys such as Ti6Al4V, there is a risk of aluminium and vanadium ions getting into the tissues around the implant and the bloodstream. The release of these metal ions can cause irritation of the tissues surrounding the implant, and by getting into the bloodstream, it can cause cytotoxic reactions and neurogenic disorders **[L. 3–6]**. Surface modification treatments are used to eliminate the problem of ion release and improve the properties of titanium and its alloys. Any surface treatment can be applied that improve the functional properties and provide a positive tissue response around the implanted implant.

Currently, the modification of the surface layer through various types of physicochemical treatments, deposition of surface layers and coatings and ion implantation **[L. 1]** are increasingly popular. Initially, implantation was used only in nuclear physics; however, over time, it has found application in various industries, e.g., in electronics, material engineering, and medicine. It is used both to modify the surfaces of metals, ceramics and polymers **[L. 7–9]**. Ion implantation is a process involving the introduction of ions of any element, regardless of the conditions and thermodynamic limitations, into the subsurface surface layer. Ions penetrate the structure of the material due to the high kinetic energy acquired in the electric field accelerating them. As a result of implantation, the atoms of the parent material and the implanted ions are "mixed". The process diagram is shown in **Fig. 1**.

The energy of the implanted ions is usually in the range from a few keV to several MeV, while the thickness of the implanted layers ranges from a fraction of to a few micrometres **[L. 10–12]**. Due to the fact that in the process of ion implantation there is no application of an additional layer (as in the case of coatings), the problem of adhesion between the modified layer and the material core was eliminated. Undoubtedly, this is a great advantage, because peeling or crumbling of the coating is a frequent problem that occurs during the exploitation period **[L. 13]**. Another strength of the technology is the low temperature of the process, which does not cause changes in the structure of the implanted material, thus retaining high process purity and high control over the process, because it is possible to adjust the implantation energy and ion dose. Despite its many advantages, the technology also has disadvantages. The largest of these is the high cost of the process, which means that it can only be used in large-scale production or where it is impossible to produce materials with the desired properties using other, cheaper methods **[L. 14, 15]**. Despite many existing surface engineering techniques, ion implantation is one of the most advanced methods of material surface modification.

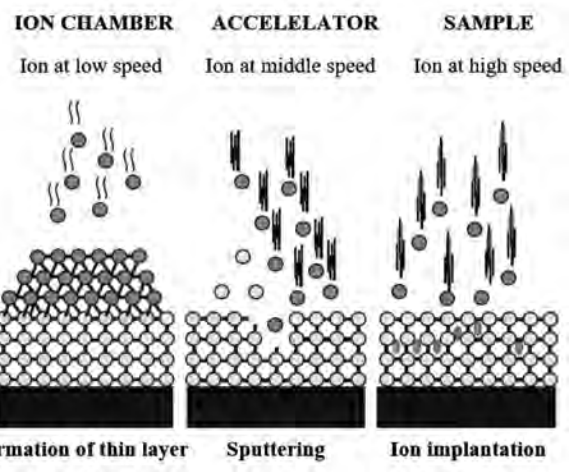

Fig. 1. Diagram of ion implantation
Rys. 1. Schemat implantacji jonowej

Due to the growing demand for biomaterials, the aim of this study was to obtain the ion implantation technique of surface layers consisting of argon or nitrogen and to assess the impact of implanted ions on the properties of Ti6Al4V titanium alloy.

MATERIALS AND METHODS

Materials

The titanium alloy Ti6Al4V with the chemical composition presented in **Table 1** was tested. Its choice was dictated by the fact that it is currently one of the most popular materials used for medical implants. In addition, it is characterized by high corrosion resistance, high biocompatibility and biotolerance compared to other metallic materials **[L. 16]**.

Prior to ion implantation, the front surfaces of the 30x30x5 mm samples were ground and polished using a sander/polisher. SiC papers were used for grinding with grain gradation increasing from 120 to 2500 μm, and diamond paste with 1 μm grain gradation used for polishing. Then the samples were ion implanted. The process was carried out with the following parameters:

– Ion dose: $5x10^{17}$ N^{+}/cm^2 and $5x10^{17}Ar^{+}/cm^2$,
– Energy 35 kV.

Table 1. Chemical composition of titanium alloy Ti6Al4V, % wag.
Tabela 1. Skład pierwiastkowy stopu tytanu Ti6Al4V, % wag.

Element							
Ti	Al	V	Fe	O	C	N	H
Total	5.50-6.75	3.5-4.5	Max. 0.4	Max. 0.2	Max. 0.08	Max. 0.05	Max. 0.015

Methods

The geometric structure of the surface before (**Fig. 3**) and after the tribological tests (**Figs 12–13**) was analysed using a confocal microscope with the Leica DCM8 interferometric mode. During the tests, the most important parameters of the geometric structure of the surface were determined (**Table 3**) and the depth and the abrasion area on the cross-section was measured.

The hardness of the tested materials was determined using an Anton Paar micro hardness tester using the instrumental indentation method. The test consisted of pressing a Vickers, 250 nm radius indenter into the material **[L. 5]**. The measurement was performed with a nominal loading force of 2 N and a rise speed of 4000 mN/min. This advanced research technique allowed precise recording of the load curve and the penetration depth of the indenter.

The tribological tests were carried out on a ball-on-disc NTR nanotribometer (**Fig. 2**) in a reciprocating motion. The tests were carried out in conditions of dry friction and friction with Ringer's solution lubrication, with technical and environmental parameters presented in **Table 2**. The counter-sample in the tested friction nodes was a ball made of aluminium oxide (III) with a diameter of 2 mm (Ra 0.37 μm). An amplitude of 1 Hz and a load of 50 mN were used.

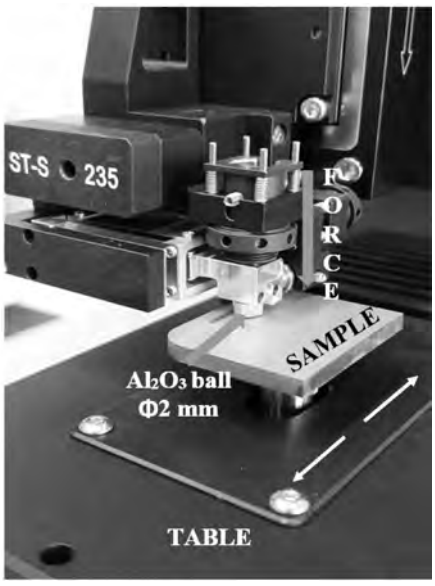

Fig. 2. View of pin on disc on the NTR
Rys. 2. Widok węzła tarcia nanotribometru NTR

Table 2. Technical and environmental parameters of test
Tabela 2. Techniczne i środowiskowe parametry testu

Parameter	Unit	Friction pair
		ballAl_2O_3 – disc Ti6Al4V ball Al_2O_3 – disc Ti6Al4V with N^+ ball Al_2O_3 – disc Ti6Al4V with Ar^+
Load	mN	50
Linear speed	m/s	0.0159
Cycle	–	10 000
Frequency	Hz	1
Humidity	%	50 ±1
Temperature	˚C	23 ±1
Lubricant	–	without Ringer solution

Scanning electron microscopy using Phenom XL was used to observe the surface morphology after tribological tests. The measurement was carried out with an accelerating voltage of 15 kV at magnifications of 1000x, 3000x, and 5000x.

RESULTS AND DISCUSSION

The first stage of the research was to evaluate the geometric structure of the surface after implantation with nitrogen and argon ions. **Figure 3** shows isometric images with the primary surface profile. Additional information was obtained from the values of the amplitude parameters (**Tab. 3**).

The isometric images, primary profiles, and the values of the most important amplitude parameters (Ra, Rp, Rv, Rz) presented in **Fig. 3** indicate changes in the geometric structure of the surface of the tested samples after the ion implantation process. As a result of ion implantation with nitrogen ions, the roughness parameters of the samples increased by about 20%, while for samples implanted with argon ions, these values increased by 70%.

The mechanical properties of thin layers determine the durability and reliability of the elements on which they are applied. **Figure 4** shows the load-unload curves recorded during indentation. Mechanical parameters were determined based on the measurement of the penetration depth of the indenter and the knowledge of its geometry. **Table 4** presents their average values obtained from 10 measurements.

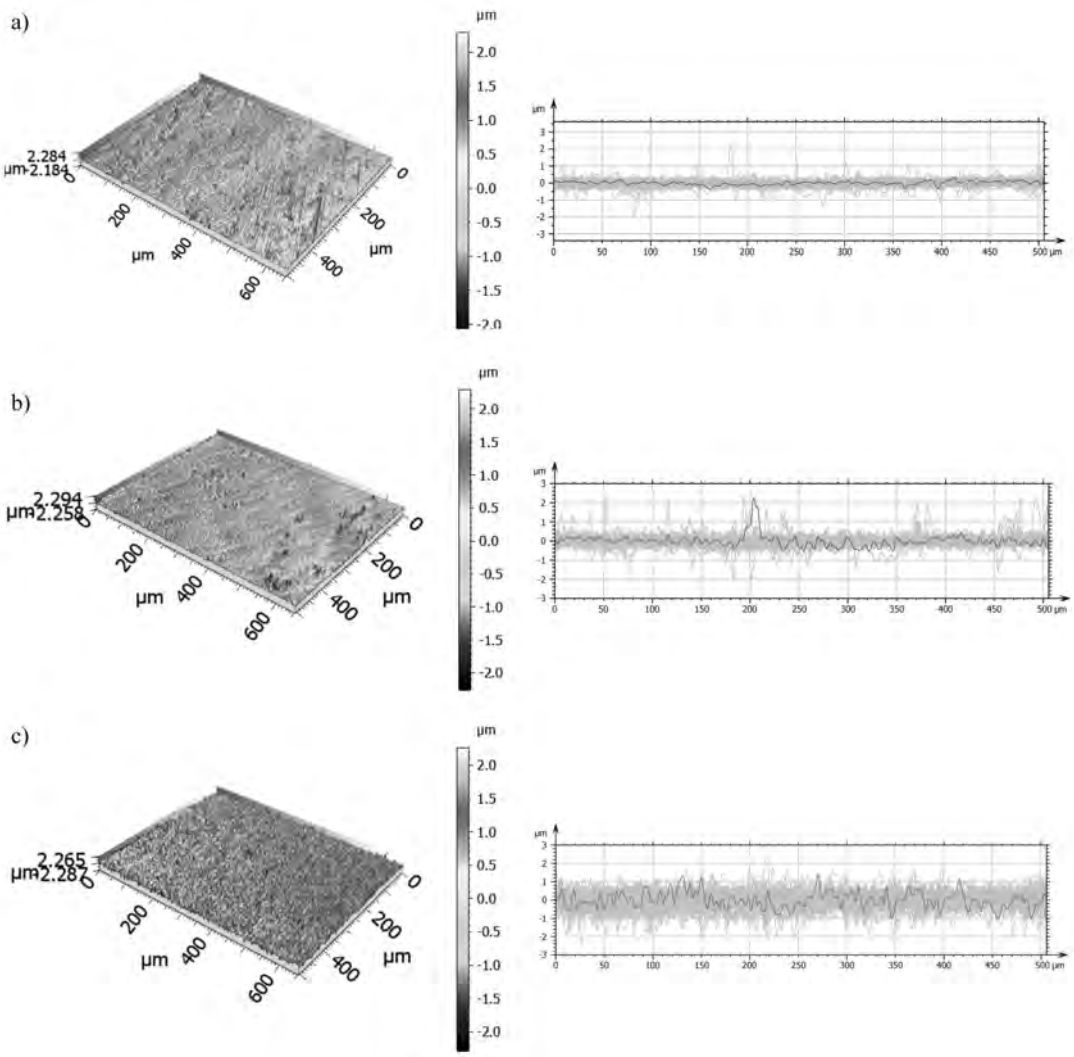

Fig. 3. Isometric images and profile of surface: a) a reference sample, b) N^+ ion implantation, c) Ar^+ ion implantation
Rys. 3. Obrazy izometryczne oraz profile powierzchni: a) próbka referencyjna, b) implantowana jonami N^+, implantowana jonami Ar^+

Table 3. Parameters of the surface geometry after ion implantation
Tabela 3. Parametry struktury geometrycznej powierzchni po implantacji jonowej

Parameter	reference sample		N^+ ion implantation		Ar^+ ion implantation	
	mean	SD	mean	SD	mean	SD
Ra [µm]	0.10	0.02	0.14	0.03	0.31	0.04
Rp [µm]	0.48	0.33	0.76	0.47	1.09	0.30
Rv [µm]	0.49	0.20	0.67	0.36	1.31	0.34
Rz [µm]	0.98	0.43	1.44	0.63	2.40	0.47
Rsk	-0.20	1.23	0.12	1.37	-0.25	0.52
Rku	6.38	5.56	7.03	6.36	3.87	1.14

The curves shown in **Fig. 4** show the high plasticity of the substrate. This is evidenced by the nature of the indentation curve slope and the obtained values of the contact area, total work, and the work of elastic and plastic deformation.

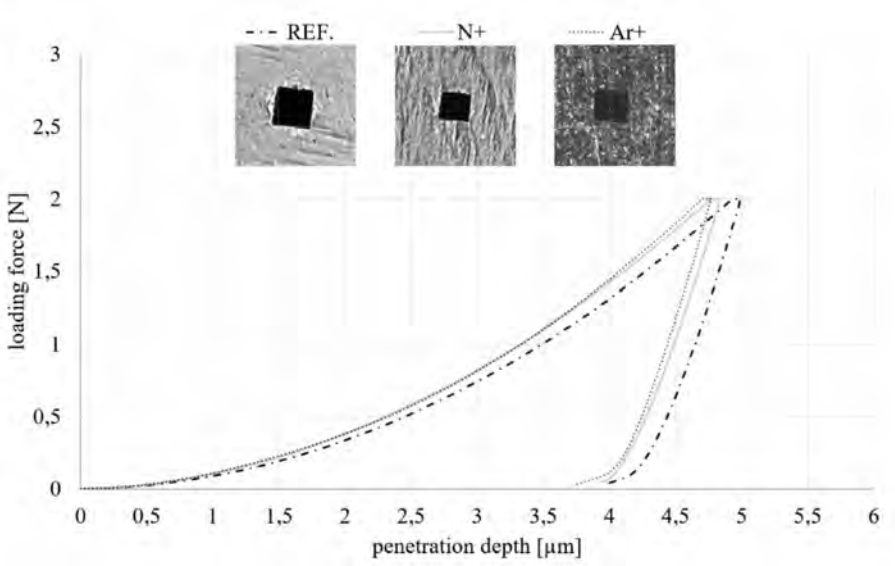

Fig. 4. Load – penetration depth curves from indentation tests for Ti6Al4V
Rys. 4. Krzywa obciążenia – głębokość penetracji wgłębnika zarejestrowana podczas testu twardości

Table. 4. Mechanical parameters
Tabela 4. Parametry mechaniczne

Parameters	Unit	Sample		
		reference sample	N^+ ion implantation	Ar^+ ion implantation
Indentation hardness [H_{IT}]	MPa	3763±14.3	4014±22.6	4071±15.8
Vickers Hardness [HV]	HV	355±13.6	381±21.1	384±14.9
Young Modulus [E^*]	GPa	134±1.2	137±3.1	141±6.7
Contact area [A_p]	μm^2	532±0.2	499±0.2	492±0.1
Plastic work [W_{plast}]	μJ	2.77±0.11	2.74±0.12	2.63±0.006
Elastic work [W_{elast}]	μJ	0.72±0.02	0.71±0.01	0.70±0.05
Total work [W_{tot}]	μJ	3.49±0.08	3.45±0.11	3.33±0.05
Maximum depth of indentation [h_m]	μm	5.1±7.7	4.8±1.2	4.7±1.0

As a result of ion implantation, there was an approx. 10% increase in hardness and approx. 5% increase in the modulus of elasticity. The ability to creep was also reduced. This is evidenced by the decrease in the value of the penetration depth increment – hm under a given load – by about 5% in the case of the sample implanted with nitrogen ions and by about 10% in the case of the sample implanted with argon ions. In addition, the use of implantation caused a decrease in the value of the Wtot indentation work and its Wplast and Welast components, which proves a reduction in the susceptibility of implanted samples to deformation as a result of operational loads. Among all the tested samples, the best mechanical characteristics were obtained for samples implanted with argon ions.

The results of the friction tests are summarized in the diagram of the friction coefficient – μ (**Fig. 5**) of the tested elements depending on the types of materials in the friction pairs and the lubricants used.

Figure 5 shows that the best tribological characteristics under the conditions of technically dry friction were obtained for the material combination of Ti6Al4V alloy implanted with $Ag^+ – Al_2O_3$ ions. The recorded course of the friction coefficient was stable throughout the test period. The average value of the coefficient μ was 0.16. In the case of the reference sample, the coefficient of friction increased sharply from cycle 1 to 50 to a value of μ = 0.65, and then it increased more gently to reach a maximum value of 0.7 in the 700 cycle. At a later stage of the test, it decreased. Around 1700 cycles, the friction coefficient stabilized to the value of 0.32. The course of the sample implanted with nitrogen ions shows that between the 2800 and 4000 cycles there was a sharp jump in the μ value.

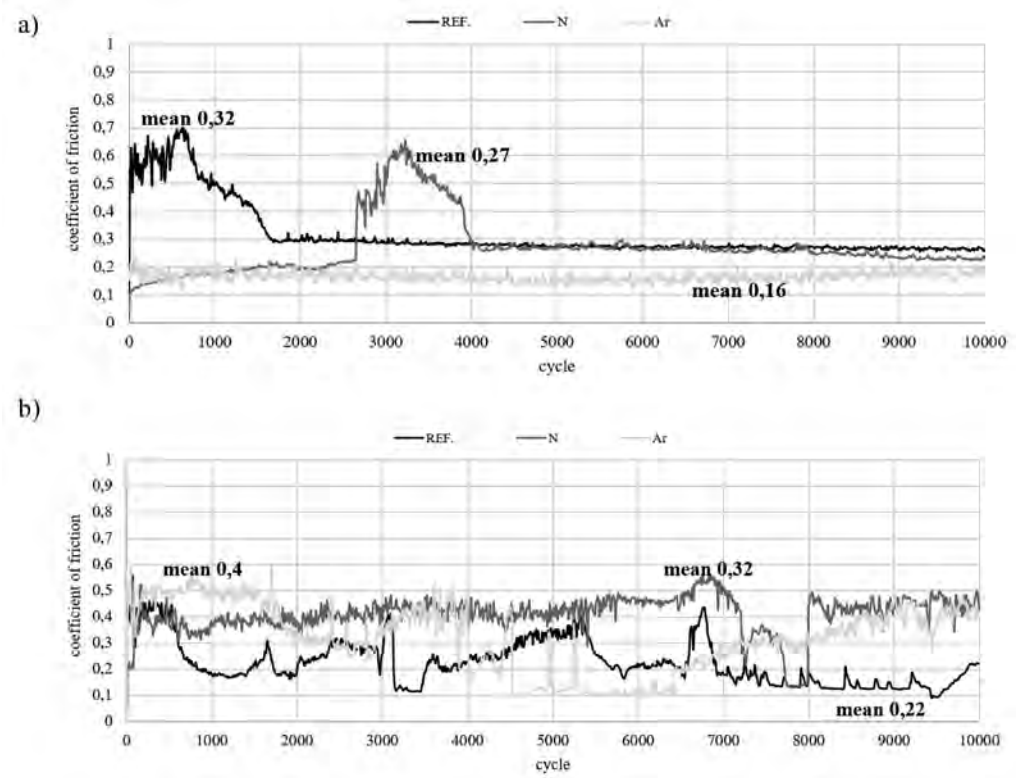

Fig. 5. Coefficient of friction during: a) technical dry friction (TDF), b) Ringer solution (RS)
Rys. 5. Współczynnik tarcia zarejestrowany podczas: a) tarcia technicznie suchego (TDF), b) tarcia ze smarowaniem roztworem Ringera (RS)

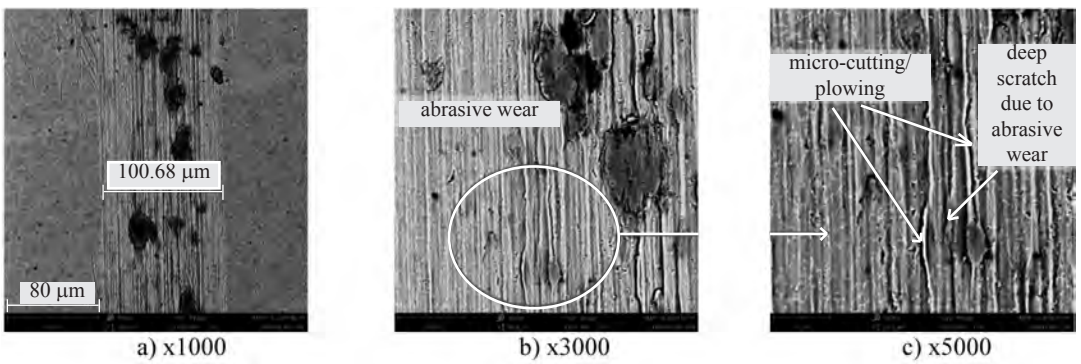

Fig. 6. Surface morphology of the wear traces after technical dry friction for a reference sample
Rys. 6. Morfologia powierzchni śladu wytarcia próbki referencyjnej po tarciu technicznie suchym

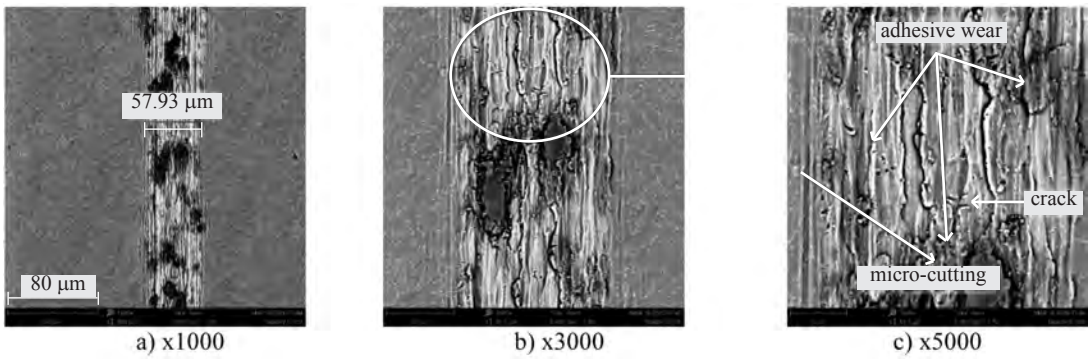

Fig. 7. Surface morphology of the wear traces after technical dry friction for N^+ ion implantation
Rys. 7. Morfologia powierzchni śladu wytarcia próbki implantowanej jonami azotu po tarciu technicznie suchym

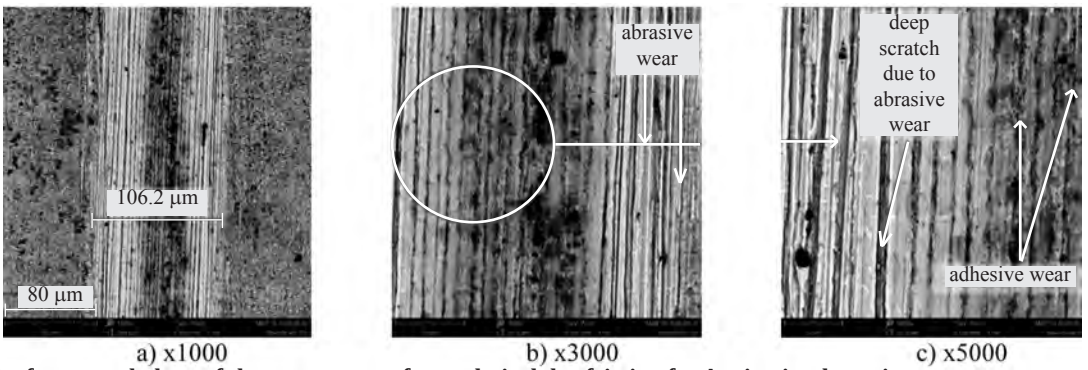

Fig. 8. Surface morphology of the wear traces after technical dry friction for Ar^+ ion implantation
Rys. 8. Morfologia powierzchni śladu wytarcia próbki implantowanej jonami argonu po tarciu technicznie suchym

Fig. 9. Surface morphology of the wear traces after friction with Ringer's solution for a reference sample
Rys. 9. Morfologia powierzchni śladu wytarcia próbki referencyjnej po tarciu ze smarowaniem roztworem Ringera

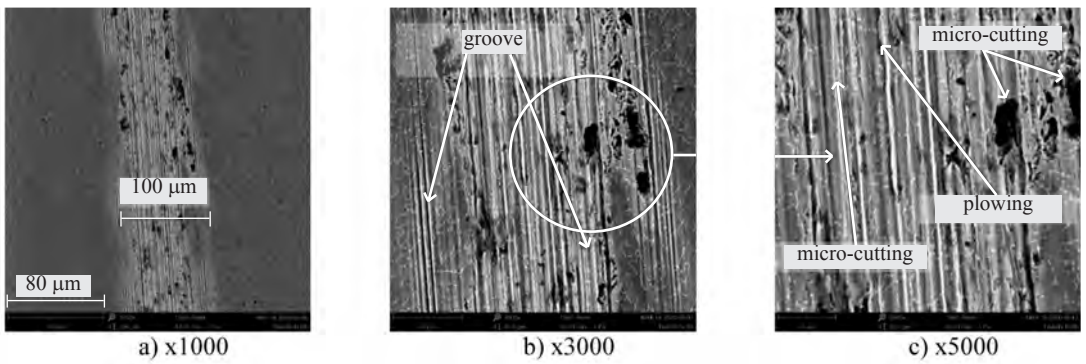

Fig. 10. Surface morphology of the wear traces after friction with Ringer's solution for N^+ ion implantation
Rys. 10. Morfologia powierzchni śladu wytarcia próbki implantowanej jonami azotu po tarciu ze smarowaniem roztworem Ringera

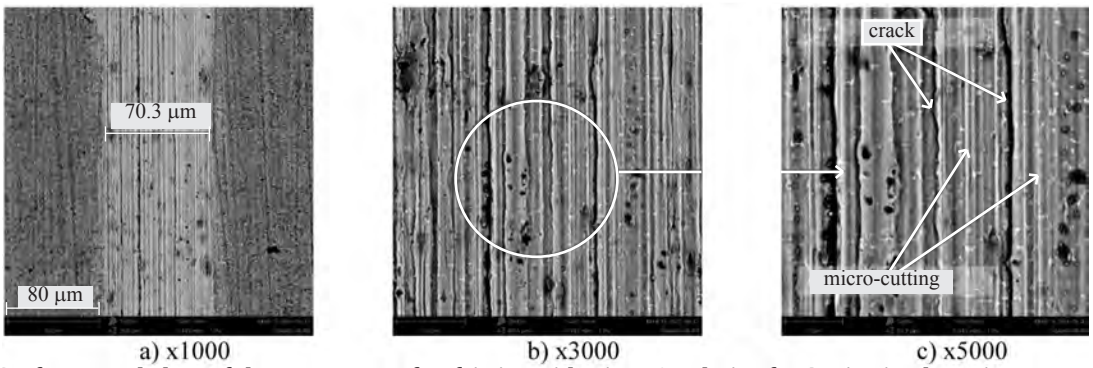

Fig. 11. Surface morphology of the wear traces after friction with Ringer's solution for Ar^+ ion implantation
Rys. 11. Morfologia powierzchni śladu wytarcia próbki implantowanej jonami argonu po tarciu ze smarowaniem roztworem Ringera

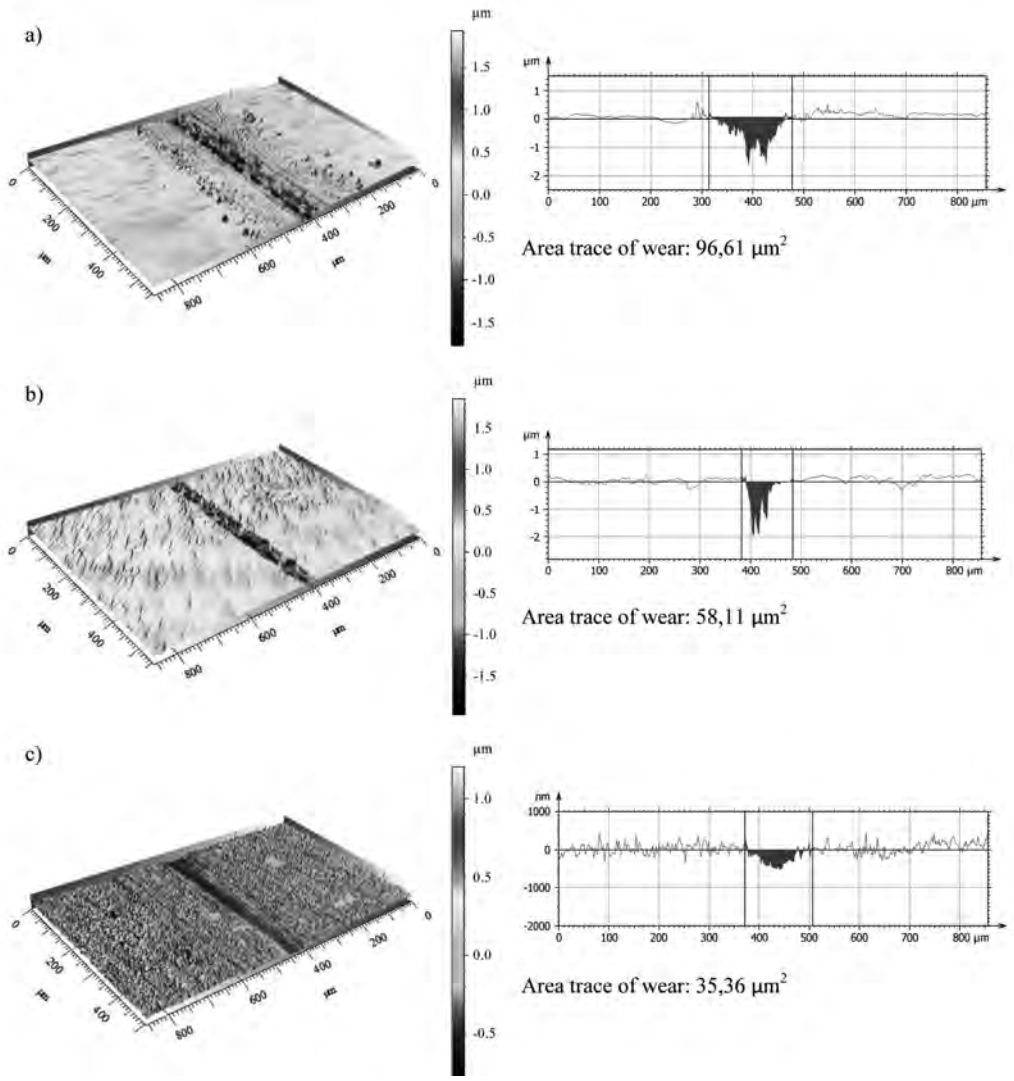

Fig. 12. The isometric image of the trace of wear and the wear profile in a cross-section for Ti6Al4V after technical dry friction: a) a reference sample, b) N^+ ion implantation, c) Ar^+ ion implantation

Rys. 12. Obraz izometryczny śladu wytarcia oraz profil wytarcia na przekroju poprzecznym po tarciu technicznie suchym a) próbka referencyjna, b) implantowana jonami N^+, c) implantowana jonami Ar^+

Most likely, at the sample-counter-sample interface, wear products appeared, which were removed from the friction zone after about 1200 cycles, and the coefficient stabilized at a value of about 0.3. In the case of friction with the use of a lubricant, very violent courses were recorded. This is due to the tribocorrosive nature of chloride ion interactions in the friction couple. The value of the friction coefficient oscillated between 0.1 and 0.6. Determination of the mean values allowed to state that the reference sample had the lowest resistance to motion.

After the tribological tests, the surface morphology of the abrasion marks was examined (**Figs 6–11**). This made it possible to determine the amount of wear and the wear mechanism.

The analysis of wear marks (**Figs 6–11**) shows that the abrasive wear mechanism dominates in all tested materials. Its occurrence is related to the several times greater hardness of the Al_2O_3 counter-sample than the tested samples. Cracks and furrows visible in the SEM images were created as a result of the movement of loose wear products in the area of the friction zone. The modified top layer, i.e. after implantation with Ar^+ ions, was completely destroyed and removed during friction, which is indicated by a deep and wide abrasion mark. In the case of Ti6Al4V implanted with N^+ ions, the measured abrasion marks were smaller, their width oscillated between 50–110 µm. Counter-samples were also tested – balls made of Al_2O_3, on which no signs of wear were observed.

After tribological tests, the samples were measured for wear traces. **Figures 12–13** show isometric images and wear profiles of the test wheels. The wear area on

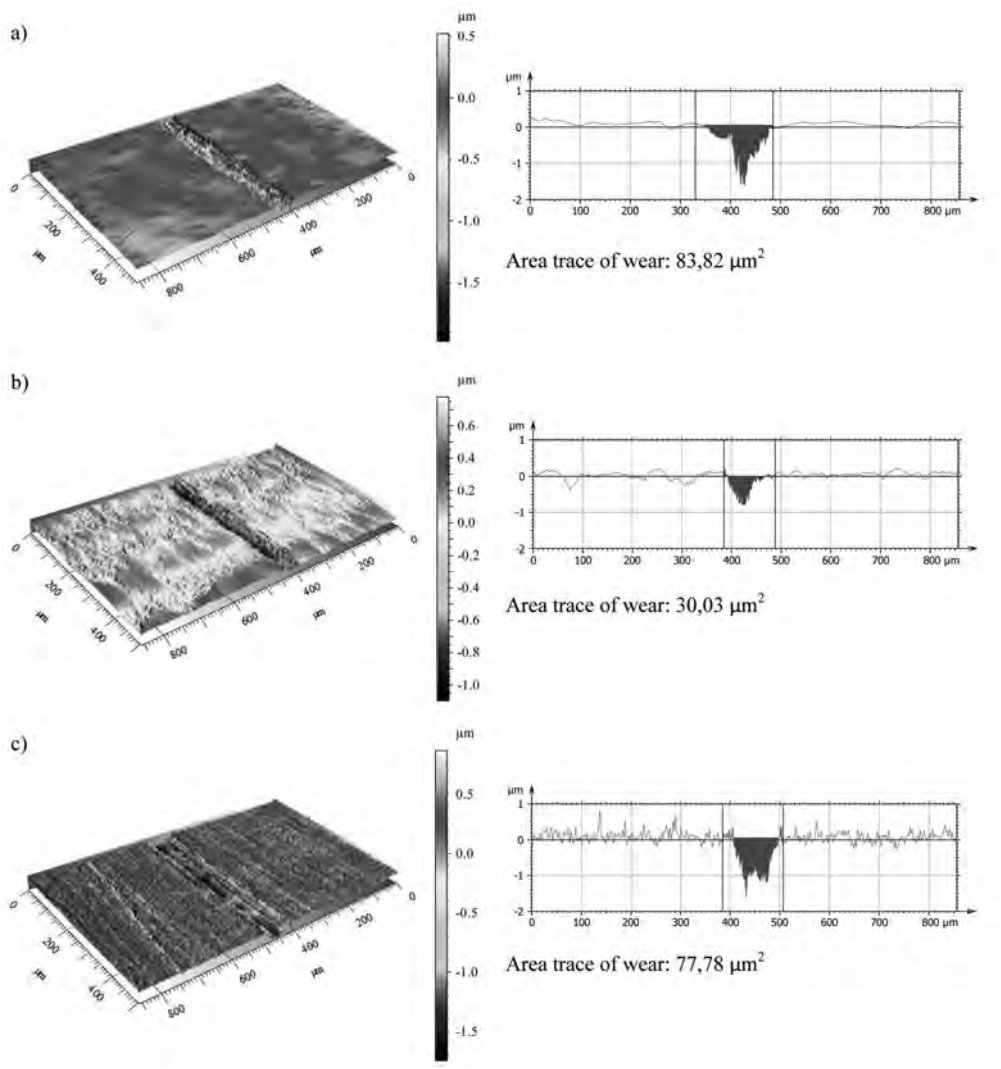

Fig. 13. The isometric image of the trace of wear and the wear profile in a cross-section for Ti6Al4V after friction with Ringer's solution: a) a reference sample, b) N^+ ion implantation, c) Ar^+ ion implantation

Rys. 13. Obraz izometryczny śladu wytarcia oraz profil wytarcia na przekroju poprzecznym po tarciu ze smarowaniem roztworem Ringera a) próbka referencyjna, b) implantowana jonami N^+, c) implantowana jonami Ar^+

the cross-section was adopted as a measure of wear. Observations of counter-samples – balls revealed no traces of wear.

The results of the research on the geometric structure of the surface after tribological tests showed an increase in wear resistance through friction of the implanted samples. This phenomenon is most noticeable during technically dry friction. Among all the studied cases, it was noticed that the sample implanted with argon ions was used up the least. The resulting wear area was 65% lower compared to the result obtained for the Ti6Al4V substrate. The analysis of wear marks examined after friction with Ringer's solution lubrication showed that Ti6Al4V implanted with nitrogen ions is characterized by the highest wear resistance. Approximately 70% and 60% lower wear areas were noted for the Ti6Al4V and Ti6Al4V alloys implanted with argon ions, respectively. The results of hardness tests showed that ion implantation improves the mechanical properties. There was an increase of about 10% in hardness and a 5% increase in Young's modulus.

CONCLUSIONS

At the same time, the modification of the surface layer with N^+ and Ar^+ ions caused a decrease in the value of the indentation work. This reduces the susceptibility of implanted samples to deformation as a result of operational loads. Among all tested materials, the best mechanical parameters were obtained for the sample implanted with Ar^+ ions. The results of the friction

tests carried out in dry friction conditions revealed a stable course of the friction coefficient practically throughout the entire duration of the test. In the case of friction with lubricant, the course was more turbulent. The obtained tribological characteristics indicate that, during technically dry friction, the implanted surfaces, both with argon and nitrogen, were characterized by a lower average coefficient of friction than the reference surfaces, and the lowest wear was obtained for surfaces implanted with argon ions. On the other hand, in the case of friction with the lubrication of Ringer's solution, higher mean values of the coefficients of friction of the implanted surfaces were recorded than for the reference sample, with simultaneously recorded lower abrasion fields of the implanted samples. The analysis of the surface of the wear marks revealed that the nature of the wear of all tested samples indicates a typical abrasive wear mechanism. Cracks and furrows visible in the SEM images were created as a result of the movement of loose wear products in the area of the friction zone. Microcracks were also observed in the traces of wear. The analysis of the geometrical structure of the surface showed that, in almost all the tested nodes of friction, uneven wear of the surface layer took place, and the most wear-and-tear material was the Ti6Al4V alloy.

REFERENCES

1. Liu W., Liu S., Wang L.: Surface modification of biomedical titanium micromorphology, microstructure evolution biomedical applications, Coatings, 9, 249, 2019.
2. Niemczewska-Wójcik M., Mańkowska-Snopczyńska A., Piekoszewski W.: The tribological research of materials for use in a medical technique, Tribologia, 4, 2015, pp. 111–122.
3. Loska S., Szewczenko J., Held-Tyrlik J., Paszenda Z.: Biocompatibility of surface modified Ti6Al4V ELI alloy tested in SBF, Engineering of Biomaterials, 2011, pp.154–158.
4. Marciniak J.: Biomateriały metalowe – kierunki i prognozy rozwojowe, Advanced forming technologies and nanostructured materials, Conference Proceedings, Poznań, 2012.
5. Blumenthal N.C, Cosma V.: Inhibition of apatite formation by titanium and vanadium ions, J Biomed Mater Res., 1989, 23, pp.13–22.
6. Rautray T.R., Narayanan R., Kim K-H.: Ion implantation of titanium based biomaterials, Progress in Materials Science, 2011, 56, pp. 1137–1177.
7. Pieczyńska D., Ostaszewska U., Jagielski J., Bielinski D.M.: Modyfikacja polimerów za pomocą bombardowania jonowego Cz. I, Polimery, 56, 2011, pp. 439–451.
8. Jagielski J.: Friction properties of ion-beam modified materials: Where can we search for practical applications of ion implantation? Vacuum, 78, 2005, pp. 409–415.
9. Vaideeswaran K., Bohlen A., Wattenhofer T., Michl T., Yamahata C., Biselli S., Spoerl C., Griesser H., Sereda O., Dadras M.: Improvement of wear resistance of PEEK through multicharge ion implantation, Conference: Meet to Expert, CSEM Idonus, Switzerland, 2018.
10. Pawelec K., Baranowicz P., Wysokińska-Miszczuk J., Madej M., Skóra M.: The tribological properties of the Ti6Al4V alloy with nitrogen ion implantation, Tribologia, 1, 2019, pp. 37–47.
11. Rautray T.R., Narayanan R., Kim K.H.: Ion implantation of titanium based biomaterials, Progress in Materials Science, 56, 2011, pp. 1137–1177.
12. Kamioński M., Budzyński P.: Implantacja jonowa jako sposób konstytuowania warstwy wierzchniej podzespołów silników spalinowych, 12, 2017.
13. Burnat B., Błaszczyk T., Leniart A.: Anticorrosion properties of TiO_2 SOL-GEL coating in relation to PH of solution and presence of serum protein, Engineering of biomaterials, 122–123, 2013, pp. 50–55.
14. Jagielski J., Piatkowska A., Aubert P., Thomé L. et al.: Ion implantation for surface modification of biomaterials. Surface and Coatings Technology, 200, 2006, pp. 6355–6361.
15. Tarnowski M., Garbacz H., Ossowski M., Wierzchoń T.: Kształtowanie właściwości użytkowych stopu tytanu Ti6Al4V w niskotemperaturowym procesie azotowania jarzeniowego. Inżynieria Materiałowa, 35, 2014, pp. 420–422.
16. Sulej-Chojnacka J., Wielowiejska-Giertuga A., Mróz A., Delfosse D.: Fretting corrosion of cobalt and titanium implant alloys in simulated body fluids, Tribologia, 6, 2016, pp. 149–158.